Noname manuscript No.
(will be inserted by the editor)

Multivariate Risk Analysis in Cryptocurrency Market: An Optimal Transport Approach

João Pedro M. Franco · Márcio Laurini*

Received: date / Accepted: date

Abstract This study explores the cryptocurrency market by applying novel multivariate risk measures grounded in optimal transport theory to estimate Vectors-at-Risk (VaR) and Conditional-Vectors-at-Risk (CVaR). We compare the results of this approach with traditional univariate methods for estimating Value-at-Risk and Conditional Value-at-Risk, evaluating factors such as magnitude, computational time, and backtesting performance. Our findings indicate that although this new method incurs substantially higher computational costs, it effectively incorporates the correlation structure among assets' risks, yielding more conservative estimates than conventional tail risk estimation techniques.

Keywords Tail Risk · Criptocurrencies · Optimal Transport · Superquantiles · Backtesting.

João Pedro M. Franco · Márcio Laurini
FEARP - University of São Paulo, Brazil - Av. dos Bandeirantes 3900, 14040-905, Ribeirão Preto, SP, Brazil
Tel.: +55-16-33290867
*Corresponding author - Márcio Laurini - E-mail: laurini@fearp.usp.br
The authors acknowledge funding from Capes, CNPq (310646/2021-9) and FAPESP (2023/02538-0). Declarations of interest: none

1 Introduction

Cryptocurrencies have received greater attention from investors, regulators, and policymakers in recent times, with market capitalization reaching USD 2.23 trillion on 2022/01/05 (Akhtaruzzaman et al., 2022). There are several reasons for this growth. Firstly, the utilization of decentralized blockchain networks eliminates the need for intermediaries such as banks or financial institutions. Additionally, cryptocurrency markets operate around the clock, enabling accessibility to anyone with an internet connection. Furthermore, cryptocurrencies present diversification opportunities for investors seeking to hedge against traditional financial assets such as stocks and bonds. In addition, the increase in regulatory clarity and institutional adoption has bestowed legitimacy upon the cryptocurrency market.

Cryptocurrency markets are characterized by high volatility, leading to sudden price fluctuations (Chaim and Laurini, 2018). This volatility, coupled with media hype and speculation, creates an environment ripe for speculative activities, attracting traders seeking short-term gains. However, the inherent risk associated with cryptocurrencies is amplified by their extreme volatility. Consequently, in the context of a cryptocurrency portfolio, assessing joint risk is essential (Borri, 2019).

Bercu et al. (2023) argues that univariate measures of risk fail to capture the correlation structure between the components of a random vector, necessitating the use of multivariate measures. Bercu et al. (2023) emphasizes that vector-valued risk measures are robust candidates for encompassing all tail distribution information, including direction and spread. Both Galichon (2017) and Bercu et al. (2023) highlight several studies that seek to provide generalizations for the multivariate case (Cai et al., 2022; Cousin and Di Bernardino, 2014, 2013; Heffernan and Tawn, 2004; Prékopa, 2012; Torres et al., 2015).

However, as highlighted by Bercu et al. (2023), none of these measures explore the properties of optimal transport theory, specifically the characteristics of Monge-Kantorovich quantiles. These quantiles do not require any assumptions about the distribution's tail or statistical model. This gap exists because Monge-Kantorovich quantiles are highly adaptable in adjusting to the distribution's shape.

Tail risk measures are typically characterized in terms of the extreme quantiles of the distribution. However, the main limitation of these concepts is due to the fact that they are hard to be extended when dimension $d \geq 2$, in other words, in the multivariate case. Hallin et al. (2021) point that the empirical versions (empirical quantiles and ranks) of multivariate distributions are fundamental in statistical inference, and any multivariate extension that does not enjoy, in dimension $d \geq 2$, the properties that dimension $d = 1$ offers, is not a desirable statistical extension.

As discussed in Del Barrio et al. (2019), this issue is longstanding, and numerous studies have attempted to define multivariate versions of distribution and quantile functions using classical rank- and quantile-based inference techniques. Some studies investigate the concept of data depth, as seen in

works such as Liu (1990), Oja (1983), and Zuo (2003). A geometric approach is analyzed in Chaudhuri (1996), Hallin et al. (2010), and Koltchinskii (1997). Nevertheless, these new definitions do not offer the useful properties of univariate ranks and univariate quantiles and, one problem, emphasized by Ghosal and Sen (2022), is that these notions can lead to values outside the support of the distribution.

However, Ghosal and Sen (2022) point out that the optimal transport theory can extend the univariate properties of quantiles and ranks to the multivariate case. The main objective of optimal transport theory/Monge´s problem is to find a measurable transport map $T \equiv T_{\mu;\nu} : \mathcal{S} \to \mathcal{Y}$ that solves a constrained minimization problem. Based on the theory of optimal transport, the concepts of center-outward multivariate ranks and signs were introduced in Hallin et al. (2021). Hallin et al. (2023) argues that center-outward ranks and signs have, when the dimension is $d > 1$, the same properties as traditional univariate ranks, case where $d = 1$ and, moreover, are distribution-free.

Bosc and Galichon (2014) describe a generalized methodology of extreme multivariate dependence between two random sets, which is based on the extremality of the cross-covariance matrix and has applications in risk management. Ekeland et al. (2012) proposes a multivariate extension of the notion of comonotonicity involving simultaneous optimal rearrangements between two vectors of risk. Extending these ideas to the cases of vector-valued Y, with values in $\mathbb{R}^d$, Carlier et al. (2016) propose a conditional vector quantile function and also a vector quantile regression, which embeds the classical Monge-Kantorovich optimal transportation problem at its core as a special case.

Bercu et al. (2023) explore the probability tails related to high values of each component, which is located in the center-outward quantiles and superquantiles. Once we have the center-outward contours, Bercu et al. (2023) shows that the Vector-at-Risk and Conditional-Vector-at-Risk (as known as Expected Shortfall, Superquantile or even Expected Tail Loss) of order α, which can be define as, respectively, the most extreme risk and the average risk beyond this most extreme risk, can be calculated. In this way, Bercu et al. (2023) calculates multivariate probability tails using superquantiles to complement the information obtained with quantiles. Rockafellar and Royset (2013) point out that superquantiles, unlike conventional quantiles, have properties of coherence and regularity, which makes the superquantile an adequate scalar representation of a random variable in a risk market.

As pointed out by de Valk and Segers (2018b), the study of tail regions of probability distributions has important applications in financial markets. In this vein, we implement the methodology proposed by Bercu et al. (2023) in the cryptocurrency market, to analyze the multivariate tail risk among the larger cryptocurrencies in terms of market capitalization (data from `coinmarketcap.com`): BTC, ETH, BNB, XRP.

This study has two main motivations. The first one is about the potential applications of optimal transport methods in financial markets, mainly in risk management measures, as indicated by Hallin et al. (2021). The second one,

more specifically, is to analyze how this method performs in a market that has really extreme risks and returns, the cryptocurrency markets.

Tail risk modeling in cryptocurrencies is made difficult by the specific characteristics of this market. Volatility is much higher than in traditional markets such as stocks, which can be explained by the presence of discontinuous price variations, linked to occurrences of jumps in the mean and variance (Chaim and Laurini, 2019a,b). This market is also characterized by the presence of dependency structures in skewness and kurtosis, which makes it quite difficult to choose an appropriate distribution for parametric modeling of tail risk, as discussed in Vieira and Laurini (2023). Also, there is evidence of non-linear patterns of dependence on tail events in the cryptocurrency market (Naeem et al., 2020; Jlassi et al., 2023; Mensi et al., 2023).

Therefore, our approach to calculating risk measures derived from the Optimal Transport theory analyzes whether the more robust and adaptable nature of this method is capable of representing these stylized facts of the cryptocurrency market. The use of measures such as Vectors-at-Risk and Conditional Vectors-at-Risk built using tail event representations derived from Optimal Transport theory can be a relevant addition to risk estimation and management tools in this market.

We also compare the results obtained by the Optimal Coupling model with other methods used for estimating static tail risk measures, such as Monte Carlo simulation, Historical Simulation, and the Variance-Covariance method, which have become prevalent since the 2009 financial crisis, as noted by Shayya et al. (2023). These methods are compared both in-sample and through backtesting procedures.

This paper is structured as follows. Section 2 presents the methodology to be estimated, Section 3 describes the data set, Section 4 presents and discusses our main results. Section 5 concludes.

2 Methodology

As risk measures derived from optimal transport theory are not yet commonly used in risk management, we review the fundamental concepts of this methodology in this section. Denote X as an integrable absolutely continuous random variable with cumulative distribution function F. The quantile function (e.g., Koenker, 2005) is

$$Q(\alpha) = F^{-1} = \inf\{x : F(x) \geq \alpha\}, \tag{1}$$

where α is the quantile for $0 < \alpha < 1$. Note that the best-known risk measure, Value-at-Risk, is the quantile of the distribution. As pointed out by Rockafellar et al. (2014), the conventional quantile is a problematic risk measure in the coherence sense and also does not have the sub-additive property (Embrechts, 2000). In other words, it is possible for a quantile of the sum of two random variables to exceed the sum of the quantiles of each individual random variable at the same probability level. This observation, as noted by Rockafellar et al.

(2014), challenges the conventional understanding of risk, which generally emphasizes diversification in portfolio management.

Acerbi and Tasche (2002) point out that the Expected Shortfall and Superquantiles complement the information obtained with conventional quantiles. The Superquantile $S(\alpha)$ and Expected Shortfall $\mathbb{E}(\alpha)$ functions are defined by Bercu et al. (2023) in the following manner

$$S(\alpha) = \mathbb{E}[X|X \geq Q(\alpha)] = \frac{\mathbb{E}[X1_{X \geq Q(\alpha)}]}{\mathbb{P}(X \geq Q(\alpha))} = \frac{1}{1-\alpha}\mathbb{E}[X1_{X \geq Q(\alpha)}], \tag{2}$$

$$E(\alpha) = \mathbb{E}[X|X \leq Q(\alpha)] = \frac{\mathbb{E}[X1_{X \leq Q(\alpha)}]}{\mathbb{P}(X \leq Q(\alpha))} = \frac{1}{\alpha}\mathbb{E}[X1_{X \leq Q(\alpha)}]. \tag{3}$$

Bercu et al. (2023) point for the fact that $S(\alpha)$ and $E(\alpha)$ focus, respectively, on the upper tail and the lower tail of the distribution of X. It is important to note that superquantile can be seen as an alternative for Conditional Value-at-Risk or even the Expected Shortfall (Rockafellar and Royset, 2018; Acerbi and Tasche, 2002; Rockafellar and Royset, 2013; Bercu et al., 2023; Rockafellar et al., 2014).

Another point about superquantiles is that they can be easily implemented in stochastic optimization models and, under parametric perturbations, the superquantile of a random variable is more stable than its respective quantile (Rockafellar and Royset, 2013; Rockafellar et al., 2014). This occurs due to the fact that superquantiles of a random variable X are defined as the integral of the corresponding quantiles with respect to the probability level, i.e., the averages of the quantile measures. Furthermore, as highlighted by Rockafellar and Royset (2013), superquantiles have two properties that conventional quantiles do not offer: coherency and regularity. With these two properties, superquantiles can be seen as a suitable scalar representation of a random variable in a risk market.

2.1 Value-at-risk

Given a confidence level α and a specified time horizon the Value at Risk of an investment portfolio is the loss that the portfolio is expected to incur over that time horizon with a probability equal to or less than the chosen confidence level. This measure can be computed as the α-quantile of its return distribution in period t

$$\Pr(r_t^i \leq VaR_{\alpha,t}^i) = \alpha, \tag{4}$$

where r_t^i denotes the returns of asset i at period t.

2.2 Optimal coupling

Let $\mathcal{X}$ and $\mathcal{Y}$ be, respectively, two closed subsets of $\mathbb{R}^d$ and $\mathbb{R}^{d'}$. Consider two probability distributions P and Q with support in $\mathcal{X}$ and $\mathcal{Y}$, respectively. Galichon (2017) defines the coupling between P and Q as a joint probability distribution π on $\mathcal{X} \times \mathcal{Y}$ with marginal distributions P and Q. This means that if (X, Y) is a random vector with probability distribution π, then its projections X and Y on $\mathcal{X}$ and $\mathcal{Y}$ should be random vectors with respective probability distributions P and Q. We denote the set of couplings as

$$\mathcal{M}(P,Q) = \{\pi : (X,Y) \sim \pi \quad \text{implies} \quad X \sim P \quad \text{and} \quad Y \sim Q\}.$$

In the case of $\mathcal{X} = \mathcal{Y} = [0,1]$ and $P = Q = \mathcal{U}([0,1])$, $\mathcal{M}(P,Q)$ coincides with the copula representation. Hence, optimal coupling method can be seen as a general case of copulas which is beyond the univariate case. More details on optimal coupling methods can be found in Galichon (2018).

2.3 Monge-Kantorovich quantiles

Bercu et al. (2023) shows that the probability measure $\nu \in \mathcal{P}(\mathbb{R}^d)$ is the push-forward of $\mu \in \mathcal{P}(\mathbb{R}^d)$ by $T : \mathbb{R}^d \to \mathbb{R}^d$, denoted by $T_{\#}\mu = \nu$, where $\mathcal{P}(\mathbb{R}^d)$ is the set of all integrable probability measures on $\mathbb{R}^d$, and ν is the target distribution and, as outlined by Ghosal and Sen (2022), can be seen as the population distribution of our observed data.

Ghosal and Sen (2022) point out that the push-forward function $T_{\#}\mu = \nu$ can be seen as a quantile function if μ is a Uniform distribution ($[0,1]$). Therefore, Hallin et al. (2021) describe that the Monge-Kantorovich quantile function of a multivariate distribution ν, with respect to a reference distribution μ, is a push-forward map $Q_{\#}\mu = \nu$ and, also point that there is a convex potential $\psi : \mathbb{R}^d \to \mathbb{R}$ that satisfies $\bigtriangledown\psi = Q$ μ-almost everywhere.

As the definition of superquantile and expected shortfall depends on quantile $Q(\alpha)$, Bercu et al. (2023) point out that the Monge-Kantorovich quantile function has properties that can help define associated superquantile and expected shortfall functions. According to the McCann (1995) theorem, if μ is absolutely continuous, then a map Q exists and is unique. Also, if μ and ν have finite moments of order two, by the Brenier (1991) theorem, Q is the solution of the Monge optimal transport problem as follows:

$$Q = \arg \min_{T:T_{\#}\mu=\nu} \int_{\mathcal{X}} ||u - T(u)||^2 d\mu(u), \tag{5}$$

where $u \in \mathbb{B}(0,1) \setminus \{0\}$. Following Bercu et al. (2023), the uniform spherical distribution is chosen for μ, denoted by $\mu = U_d$. This distribution is given by the product $R\Phi$ between two independent random variables R and Φ, which is drawn, respectively, from a uniform distribution on $[0,1]$ and on the unit sphere, in a way that samples from U_d are distributed from the origin to the

outward within the unit ball. The balls of radius $\alpha \in [0,1]$ have probability α while being nested, as α grows.

Ghosal and Sen (2022) point out that the choice of a spherically symmetric distribution results in quantile maps that are equivariant under orthogonal transformations. Therefore, we have that the hyperspheres of radius α are the relevant quantile contours with respect to μ. The quantile map, Q, transports in an adequately way this center-outward ordering towards the distribution ν, since that Q is a gradient of a convex function. Q will be refered as the center-outward quantile function of ν, when $\mu = U_d$.

As pointed by Beirlant et al. (2020), the center-outward distributions and quantile functions cover the lack of left-to-right ordering in cases when $d > 1$. The center-outward ordering, as highlighted by Bercu et al. (2023), captures the support of the ν distribution and, using the function for push-forward maps, returns the quantile contours, which are indexed by a probability level $\alpha \in [0,1]$.

An important point to be noted is about deepness in the spherical uniform distribution. Bercu et al. (2023) affirm that y is deeper than x, defining as $x \geq_R y$, if the following sentence is true

$$\|Q^{-1}(x)\| \geq \|Q^{-1}(y)\|, \tag{6}$$

where $x, y \in \mathcal{X}$ and $\mathcal{X} \subset \mathbb{C}$. In this way, we find that the deeper a point is in $\mathcal{X}$, the less extreme it is with respect to ν. Furthermore, if we set $u \in \mathbb{B}(0,1) \setminus \{0\}$, $x \geq_R Q(u)$ can be rewritten, allowing us to consider observations that are more extreme than those in $Q(u)$.

Suppose $\nu \in \mathcal{P}(\mathbb{R}^d)$ be an integrable probability distribution with center-outward quantile function Q. Bercu et al. (2023) define center-outward superquantile and center-outward expected shortfall functions of ν as, respectively,

$$S(u) = \frac{1}{1 - \|u\|} \int_{\|u\|}^{1} Q\left(\alpha \frac{u}{\|u\|}\right) dt \tag{7}$$

and

$$E(u) = \frac{1}{\|u\|} \int_{0}^{\|u\|} Q\left(\alpha \frac{u}{\|u\|}\right) dt, \tag{8}$$

where $\alpha \in [0,1]$. We have that the regions and contours of such functions are, according to Bercu et al. (2023), defined as follows

- The superquantile (expected shortfall) region $\mathbb{C}^s_\alpha$ ($\mathbb{C}^e_\alpha$) of order $\alpha \in [0,1]$ is the image, denote by S (E), of the ball $\mathbb{B}(0,\alpha)$.
- The superquantile (expected shortfall) contour $\mathcal{C}^s_\alpha$ ($\mathcal{C}^e_\alpha$) of order $\alpha \in [0,1]$ is the boundary of $\mathbb{C}^s_\alpha$ ($\mathbb{C}^e_\alpha$).

2.4 Vectors-at-risk

According to Bercu et al. (2023), vectors-valued risk measures are strong candidates for multivariate risk measures, since this measures include all the information about the tails of the distribution, both in terms of spread and direction. Consider a vector of dependent losses $X \in \mathbb{R}^d$, whose unit may be different. Bercu et al. (2023) propose as measures for vector-valued risk the Vectors-at-Risk and Conditional-Vectors-at-Risk, which aim to sum up the main information contained in the center-outward quantiles and superquantiles.

For Bercu et al. (2023), since the center-outward quantile contour of order α contains the most outward points with probability α, the Vector-at-Risk of order α must belong to this contour and, also, with the assumption that each component is positive, we have that the worst vectors of losses are the furthest from the origin of the joint distribution, as well as the multivariate tails. Therefore, a maximal norm is used to select points from the center-outward quantile contour of order α.

Both measures, Vector-at-Risk and Conditional-Vectors-at-Risk at level $\alpha \in]0, 1[$, are defined as

$$\mathrm{VaR}_\alpha(X) \in \mathrm{argsup}\{\|X\|_1; X \in \mathcal{C}_\alpha\}, \tag{9}$$

$$\mathrm{CVaR}_\alpha(X) \in \mathrm{argsup}\{\|X\|_1; X \in \mathcal{C}^s_\alpha\}, \tag{10}$$

where $\|x\|_1 = \sum_{i=1}^d x_i$ on $\mathbb{R}^d$ and, $\mathcal{C}_\alpha$ is the quantile contour of order $\alpha \in [0, 1]$. Bercu et al. (2023) point out that the choice of $\|\cdot\|_1$ in the definition depends on the method of comparison of the different risks. For example, without added information, we may be induced to believe that two observations of same 1-norm have the same importance.

An interesting point is that the interpretation of Vectors-at-Risk and Conditional-Vectors-at-Risk in dimension $d > 1$, i.e., multivariate case, is the same when $d = 1$, i.e., univariate case. In other words, when $d = 1$, the VaR at level α is quantile α, while the CVaR is the superquantile of order α. In a multivariate framework ($d > 1$), Vectors-at-Risk and Conditional-Vectors-at-Risk can be understood as, respectively, the worst risk encountered with ν-probability α, and as the averaged risk beyond this quantile.

2.5 Estimation in practice

Since the Monge formulation can be highly non-linear and, also not have a unique solution, as pointed out by Ghosal and Sen (2022), we estimate the problem through the Kantorovich (1942) version, which is a more flexible formulation than the Monge problem. First, following Genevay et al. (2016), we define the set of joint probability measures on $\mathcal{U} \times \mathcal{X}$, with μ and ν being the marginal distributions, as follows:

$$\Pi(\mu,\nu) \stackrel{\text{def}}{=} \{\pi \in \mathcal{M}_+^1(\mathcal{U}\times\mathcal{X}); \forall (A,B) \subset \mathcal{U}\times\mathcal{X}, \pi(A\times\mathcal{X}) = \mu(A), \pi(\mathcal{U}\times B) = \nu(B)\}, \tag{11}$$

where $\mathcal{M}_+^1(\mathcal{U}\times\mathcal{X})$ is the set of positive random probability measures in $\mathcal{U}\times\mathcal{X}$ and, π measures the amount of mass that is moved from μ to ν, so that the π^* that optimises the problem is called optimal coupling (Genevay, 2019).

Also, following Bercu et al. (2023), the Monge-Kantorovich quantiles are estimated using an entropic map as a regularized empirical map, which allows speed up the computational estimation. The entropic optimal transport method, present in Cuturi (2013), regularizes the original problem by penalizing it with a divergence measure of the transport plan. The primal version of the problem can be structure as a regularized Wasserstein distance between an arbitrary probability measure μ and a distribution ν with finite size support J:

$$W_\epsilon(\mu,\nu) = \min_{\pi\in\Pi(\mu,\nu)} \int_{\mathcal{U}\times\mathcal{X}} c(u,x)d\pi(u,x) + \epsilon KL(\pi|\mu\otimes\nu), \tag{12}$$

where $\epsilon \geq 0$ represent the regularization parameter[1], $c : \mathcal{U}\times\mathcal{X} \to \mathbb{R}$ denote a cost function of mass transport from position u to x and, KL is a Kullback-Leibler divergence denote as

$$KL(\pi|\xi) = \int_{\mathcal{U}\times\mathcal{X}} \left(log\left(\frac{d\pi}{d\xi}(u,x)\right) - 1 \right) d\pi(u,x), \tag{13}$$

between π and a positive measure ξ on $\mathcal{U}\times\mathcal{X}$. As point out by Genevay et al. (2016) and Bercu and Bigot (2021), for $\epsilon > 0$, this problem is strongly convex and, therefore, presents a unique optimal solution for π.

As formulated by Genevay et al. (2016), the minimization problem described in Equation (12) can also be rewritten as a concave maximization problem over v only. This reparametrization is known as the semi-dual version and, for $\epsilon > 0$, the solution for the optimal transportation between μ and ν is obtained as follows.

$$W_\epsilon(\mu,\nu) = \sup_{v\in\mathcal{C}_b(\mathcal{X})} H_\epsilon(v), \tag{14}$$

$$H_\epsilon(v) = \int_{\mathcal{U}} v_{c,\epsilon}(u)d\mu(u) + \int_{\mathcal{X}} v(x)d\nu(x) - \epsilon, \tag{15}$$

[1] This regularization parameter modulates the rigidity of the constraints imposed by the optimal coupling problem. A larger regularization parameter leads to a smoother solution, potentially enhancing stability but possibly sacrificing precision in reflecting the ideal correspondence between distributions. Conversely, a smaller regularization parameter may yield a solution closer to the ideal correspondence but might be more susceptible to numerical fluctuations and instabilities.

where $\mathcal{C}_b(\mathcal{X})$ denotes the space of continuous bounded functions on $\mathcal{X}$, and $v_{c,\epsilon}(u)$ represents a smooth c-transform for v, that can be compute as follows

$$v_{c,\epsilon}(u) = -\epsilon \log \left(\int_{\mathcal{X}} \exp \left(\frac{v(x) - c(u,x)}{\epsilon} \right) d\nu(x) \right). \tag{16}$$

To formulate the problem (14) in a stochastic optimization manner, Bercu and Bigot (2021) suppose that, for any $\epsilon \geq 0$, exists v^* such that it satisfies $W_\epsilon(\mu,\nu) = H_\epsilon(v^*)$. Also, as ν is not know, Bercu and Bigot (2021) assume that

$$\nu = \sum_{j=1}^{J} \nu_j \delta_{x_j} \tag{17}$$

is a discrete probability measure which have support in $\mathcal{X} = \{x_1, \ldots, x_J\}$, where δ denotes the standard Dirac measure and the weights $\{\nu_1, \ldots, \nu_J\}$ is a known positive sequence whose sum is equal to one. Therefore, the semi-dual problem (14) can be rewritten as a correlation maximization problem:

$$W_\epsilon(\mu,\nu) = \max_{v \in \mathbb{R}^J} H_\epsilon(v), \tag{18}$$

$$H_\epsilon(v) = \mathbb{E}[h_\epsilon(\mathcal{U}, v)], \tag{19}$$

where, for $\epsilon > 0$,

$$h_\epsilon(u,v) = \sum_{j=1}^{J} v_j \nu_j - \epsilon \log \left(\sum_{j=1}^{J} \exp \left(\frac{v_j - c(u,x_j)}{\epsilon} \right) \nu_j \right) - \epsilon. \tag{20}$$

For any $v \in \mathbb{R}^J$, the function $H_\epsilon(v)$ represents the mean of $h_\epsilon(u,v)$ and u denotes a random vector sampled from the reference distribution μ. We set the regularization parameter $\epsilon = 0.001$. Therefore, the gradient vector of equation (20), for any $u \in \mathcal{U}$, is given as follows

$$\nabla_v h_\epsilon(u,v) = \nu - \pi(u,v), \tag{21}$$

where

$$\pi_j(u,v) = \left(\sum_{k=1}^{J} \nu_k \exp \left(\frac{v_k - c(u,x_k)}{\epsilon} \right) \right)^{-1} \times \nu_j \exp \left(\frac{v_j - c(u,x_j)}{\epsilon} \right), \tag{22}$$

represents the jth element of the vector $\pi(u,v) \in \mathbb{R}^J$. Thus, the gradient vector of $H_\epsilon(v)$ can be computed as

$$\nabla_v H_\epsilon(v) = \mathbb{E}[\nabla_v h_\epsilon(\mathcal{U}, v)] = \mathbb{E}[\nu - \pi(\mathcal{U}, v)] = \nu - \mathbb{E}[\pi(\mathcal{U}, v)] \tag{23}$$

Note that we have $\nabla_v H_\epsilon(v^*) = 0$ for v^* that maximizes the problem present in equation (18) since the Hessian matrix of $H_\epsilon(v)$ is, for any $v \in \mathbb{R}^J$, a negative semi-definite matrix. Therefore, to solve this problem and estimate the vector v^*, we applied the Robbins-Monro algorithm (Robbins and Monro, 1951), which is given, for all $n \geq 0$, as follows:

$$\hat{V}_{n+1} = \hat{V}_n + \gamma_{n+1} \nabla_v h_\epsilon(u_{n+1}, \hat{V}_n), \tag{24}$$

where the initial vector for v, $\hat{V}_0$, is a square integrable random vector and γ_n is a decreasing positive sequence. Bercu and Bigot (2021) shows that this structure has the almost sure convergence where

$$\lim_{n \to \infty} \hat{V}_n = v^* \quad \text{a.s.} \tag{25}$$

This convergence property guarantees the convergence of the Robbins-Monro algorithm to the entropic Kantorovich potential. Once we have v that solve the optimization problem, the entropic map can be deduced as a partial approximation of the Monge map, which is legitimated by an entropic analog of Brenier (1991)´s theorem as follows

$$Q_\epsilon(u) = \nabla \left(\frac{1}{2} \|u\|^2 - v_{c,\epsilon}(u) \right), \tag{26}$$

where $v^{c,\epsilon}(u)$ is a smooth c-transform of v as in Equation (16), for all $u \in \mathcal{U}$, and $c(u, x) = \frac{1}{2}\|u - x\|^2$. As Bercu et al. (2023) point out, the analytic form of Equation (26) is given by

$$Q_\epsilon(u) = \int_{\mathcal{X}} x g_\epsilon(u, x) d\nu(x), \tag{27}$$

$$g_\epsilon(u, x) = \frac{\exp\left(\frac{v_\epsilon(x) - \frac{1}{2}\|u - x\|^2}{\epsilon} \right)}{\int_{\mathcal{X}} \exp\left(\frac{v_\epsilon(z) - \frac{1}{2}\|u - z\|^2}{\epsilon} \right) d\nu(z)}. \tag{28}$$

The entropic map $Q_\epsilon(u)$ can be interpreted as the conditional expectation of ν w.r.t. conditional law linked to the transport plan $d\pi_\epsilon(u, x) = g_\epsilon(u, x) d\nu(x) d\mu(u)$, which represents the solution to the Kantorovich regularized problem as point out by Bercu et al. (2023). Substituting Q_ϵ into Equations (7) and (8), the following entropic analogs are obtained:

$$S(u) = \frac{1}{1 - \|u\|} \int_{\|u\|}^{1} Q_\epsilon \left(\alpha \frac{u}{\|u\|} \right) dt, \tag{29}$$

$$E(u) = \frac{1}{\|u\|} \int_{0}^{\|u\|} Q_\epsilon \left(\alpha \frac{u}{\|u\|} \right) dt. \tag{30}$$

A summarized description of the estimation process, which has been fully described in this section, is presented in Algorithm 1.

Algorithm 1: Summary of the estimation process

Input : $\epsilon = 0.001$, n_{iter}, $\hat{V}_0$, ν, J, u_0, α

Robbins–Monro algorithm:;
for { *n in (0,. . . , n_{iter})*} **do**
  Sample u_{n+1} *from* $\mathcal{U}$;
  Compute $\nabla_v h_\epsilon(u_{n+1}, \hat{V}_n) = \nu - \pi(u_{n+1}, \hat{V}_n)$;
  Update $\hat{V}_{n+1} = \hat{V}_n + \gamma_{n+1} \nabla_v h_\epsilon(u_{n+1}, \hat{V}_n)$;
end

Convergence:;
assert $\lim_{n\to\infty} \hat{V}_n = v^*$ *a.s.;*

Compute Entropic Map:;
Compute $Q_\epsilon(u) = \int_{\mathcal{X}} x g_\epsilon(u, x) d\nu(x)$;

Entropic Analogs:;
$S(u) = \frac{1}{1-\|u\|} \int_{\|u\|}^{1} Q_\epsilon \left(\alpha \frac{u}{\|u\|} \right) dt$
$E(u) = \frac{1}{\|u\|} \int_{0}^{\|u\|} Q_\epsilon \left(\alpha \frac{u}{\|u\|} \right) dt$

return $v^*, Q_\epsilon(u), S(u), E(u)$;

3 Data description

This section describes the database, which is composed of daily data on asset returns starting on 2021-07-02 and ending on 2022-09-13, for the following cryptocurrencies: Bitcoin (BTC), Ethereum (ETH), Ripple (XRP), and Binance Coin (BNB)[2]. Figure 1 shows the evolution of the returns of the chosen cryptocurrencies. In this figure we can observe the stylized facts of the cryptocurrency market, such as the large variation in returns, the presence of extreme values and the occurrence of common tail events between these assets. Table 1 summarizes the descriptive statistics for the chosen assets.

Figure 2 shows our 4-dimensional dataset, with pair scatterplots located below the diagonal and Pearson's correlation values above, while the diagonal

[2] Data on cryptocurrency returns was sourced from coinmarketcap.com

Fig. 1 Evolution of returns of the analyzed cryptocurrencies.

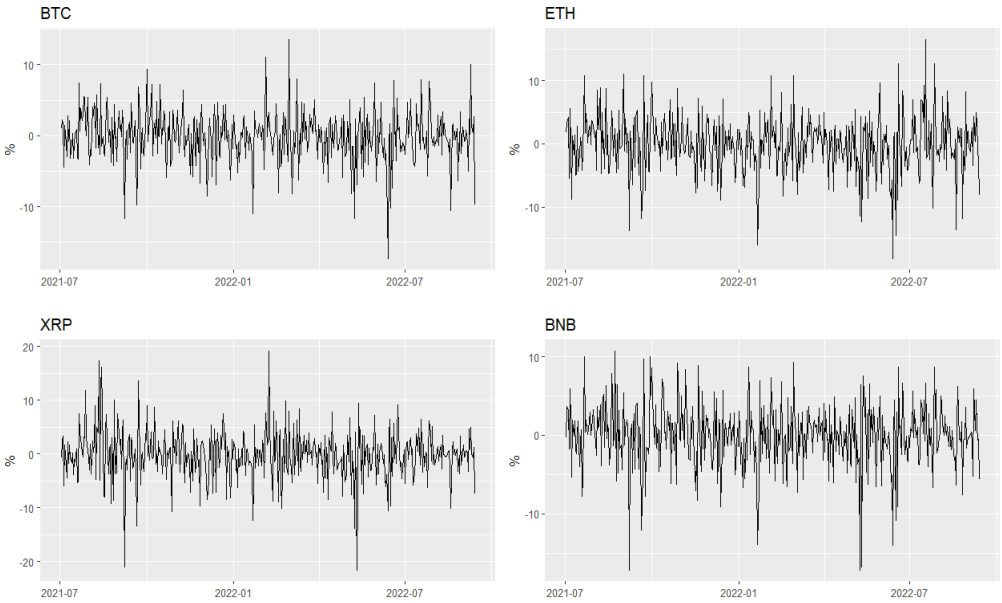

Table 1 Descriptive Statistics for cryptocurrencies (2021-07-02 to 2022-09-13)

	BTC	ETH	XRP	BNB
Mean (%)	-0.115	-0.066	-0.156	-0.009
Std (%)	3.524	4.506	4.551	4.036
Skew	-0.353	-0.232	-0.145	-0.561
Kurt	5.386	4.437	6.280	5.131
Min.	-17.405	-18.213	-21.714	-17.212
Quantile 5%	-5.908	-7.368	-7.666	-6.274
Median	-0.044	0.031	-0.050	0.099
Quantile 95%	5.232	7.035	7.235	6.466
Max.	13.576	16.496	19.135	10.725

Note: This table reports mean, standard deviation, skewness, kurtosis, minimum, quantile of 5%, median, quantile of 95% and maximum for the log daily returns on Bitcoin, Ethereum, Ripple and Binance Coin during the period of 2021-07-02 to 2022-09-13.

displays the empirical density functions of each variable. It is evident that BTC and ETH, the two largest cryptocurrencies in terms of market capitalization, have a higher correlation value (0.869) compared to other combinations among the cryptocurrencies.

4 Empirical Results and Discussion

In this section, we discuss the results regarding the optimal coupling method and consider the differences between univariate and multivariate measures.

Fig. 2 Correlations among the 4-dimensional dataset

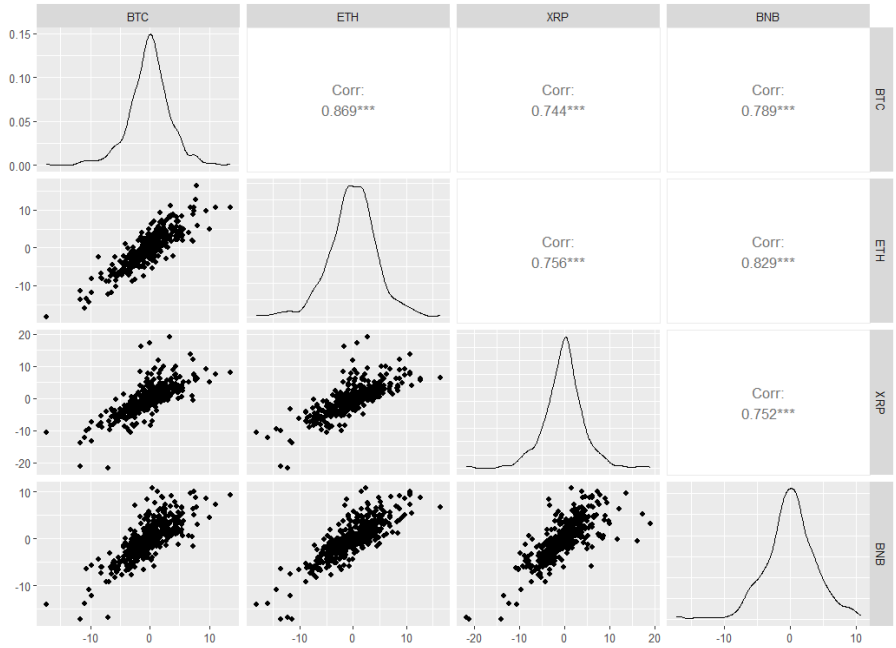

Note: This figure shows our 4-dimensional dataset, with pair scatterplots located below the diagonal and Pearson's correlation values above. The diagonal displays the empirical density functions of each variable. The p-values are represented for $^{***}p < 0.01$ $^{**}p < 0.05$ and $^{*}p < 0.10$.

Subsequently, we compare the most commonly used models for estimating univariate risk and Optimal Transport approach.

4.1 Results of Optimal Coupling methods

Tables 2 and 3 show the results for the Vectors-at-Risk and Conditional Vectors-at-Risk for the 1% and 5% quantiles for the sample analyzed. To show the problem of underestimating the risk present in the univariate measures, Table 4 summarizes the results of the univariate quantiles for the same levels indicated previously. We can observe that the results of the Vectors-in-Risk and Conditional Vectors-at-Risk estimates estimate more extreme values than the usual estimation based on the empirical quantiles of the distribution, and in this aspect, they represent a more conservative approach and adapted to the extreme values observed in this market.

The Optimal Coupling approach stands out for its ability to encapsulate the multivariate joint probability inherent in the analyzed assets, especially when considering a scenario where we're dealing with four dimensions ($d = 4$), such as BTC, ETH, XRP, and BNB. In contrast, the univariate quantile

method hinges solely on the empirical distribution of a single asset. Notably, research by Bercu et al. (2023) points out that univariate risk measures overlook the interplay between assets' correlations, underscoring the necessity for multivariate risk analysis.

To analyze these results as inputs for risk analysis, in the next section we compare these values to those obtained by traditional Value-At-Risk and Conditional Value-At-Risk calculation methods.

Table 2 Vectors-at-Risk calculated with Optimal Coupling method

	0.05	0.01
BTC	-9.285	-11.201
ETH	-12.973	-13.522
XRP	-21.414	-21.168
BNB	-16.997	-17.166

Note: This table reports the estimated Vectors-at-Risk for BTC, ETH, XRP and BNB calculated on the 5% and 1% quantiles.

Table 3 Conditional Vectors-at-Risk calculated with Optimal Coupling method

	0.05	0.01
BTC	-9.825	-11.245
ETH	-13.128	-13.535
XRP	-21.345	-21.162
BNB	-17.045	-17.170

Note: This table reports the estimated Conditional Vectors-at-Risk for BTC, ETH, XRP and BNB calculated on the 5% and 1% quantiles.

Table 4 Univariate quantiles of our variables

	0.05	0.01
BTC	-5.908	-10.454
ETH	-7.368	-13.077
XRP	-7.666	-11.740
BNB	-6.274	-13.184

Note: This table reports the estimated univariate quantiles for BTC, ETH, XRP and BNB calculated on the 5% and 1% quantiles.

4.2 Comparison with the most widely used methods for measuring risk

Shayya et al. (2023) review the models that have been applied to estimate the Value-at-Risk (VaR) in recent years, with the aim of finding the most used models after the 2009 financial crisis. In the class of static VaR estimation, the principal methods are Monte Carlo simulation, Historical Simulation and

Variance-Covariance method. Let us quickly review the techniques mentioned by Shayya et al. (2023).

As described by Danielsson (2011), the Historical Simulation approach assumes that the distribution of the returns in is time invariant, and so we can use empirical quantiles of past data as estimators to calculate the Value At Risk and the Conditional Value At Risk for future values of the return distribution. The Monte Carlo approach is based on generating a large number of future scenarios by means of random sampling. The procedure carried out in the article is to draw 1000 samples with replacement of the original data sample, and for each sample calculate the VaR and Expected Shortfall. The reported measurement is the average of these measurements across the 1000 replications performed. Note that we are in fact using the Bootstrap principle using the empirical distribution to sample from the distribution of returns.

The Variance-Covariance method (Jorion, 1996) for the Value-at-Risk estimation is made in two steps. In the first one is calculated the mean and standard deviation of the returns. The second step is to multiply the standard deviation by the desired confidence level, $\alpha(c)$, to obtain the Value-at-Risk subtracting this value of the estimated mean. This method is equivalent to assuming that the data follows a univariate Gaussian distribution (Gaussian VaR).

Tables 5 and 6 describe the Vectors-at-Risk calculated by the Optimal Coupling approach and the Value-at-Risk measured by other methods for, respectively, the 5% and 1% quantiles while Tables 7 and 8 describe the Expected Shortfall (CVaR) for the same quantiles.

Note that the Optimal Coupling and Historical Simulation approach has, respectively, in general, the highest VaR and ES (CVaR) measures, in absolute terms, among the methods analyzed with the 5% quantile. However, in the 1% quantile, the VaR and ES (CVaR) results using the Historical Simulation approach present, in absolute terms, the highest values for the measures.

As we are analyzing these results using the full sample of data, the historical method is the comparison benchmark for VaR and ES, as they are based on empirical measurements of quantiles and the average of values exceeding VaR. In this aspect, it is important to note that the Monte Carlo and Variance-Covariance methods underestimate risk measures, which can be explained by the difficulty of these methods in adequately capturing the tail risk of cryptocurrencies, which is mainly generated by very extreme values.

The Monte Carlo method is not able to adequately reproduce the probability of occurrence of these rare events, as can be seen in the discussion on the use of bootstrap methods for extreme events in Lahiri (2003). It is also evident that the Gaussian approximation is also not capable of reproducing the high tail risk that exists in cryptocurrency series. In this aspect, the Vectors-at-Risk and Conditional Vectors-at-Risk measures are capable of capturing the tail risk levels observed in the analyzed cryptocurrencies.

Therefore, these results reinforce the notion point by Bercu et al. (2023) that the optimal transport approach captures the multivariate joint probability

of the extreme events, differently the univariate methods which depend on the empirical distribution of each single asset.

Table 5 Comparing the results of Value-at-risk measure among methods for the 5% quantile

	BTC	ETH	XRP	BNB
Optimal Coupling	-9.285	-12.973	-21.414	-16.997
Historical Simulation	-10.603	-13.548	-12.366	-13.856
Monte Carlo	-5.966	-7.401	-7.726	-6.329
Variance Covariance	-5.796	-7.411	-7.486	-6.639

Note: This table reports the results of Vectors/Value-at-Risk for the methods of Optimal Coupling, Historical Simulation, Monte Carlo and Variance Covariance for the following cryptocurrencies: BTC, ETH, XRP and BNB. The results are estimated using the 5% quantile.

Table 6 Comparing the results of Value-at-risk measure among methods for the 1% quantile

	BTC	ETH	XRP	BNB
Optimal Coupling	-11.201	-13.522	-21.168	-17.166
Historical Simulation	-17.405	-18.213	-21.714	-17.212
Monte Carlo	-10.619	-13.417	-12.348	-13.697
Variance Covariance	-8.198	-10.482	-10.587	-9.390

Note: This table reports the results of Vectors/Value-at-Risk for the methods of Optimal Coupling, Historical Simulation, Monte Carlo and Variance Covariance for the following cryptocurrencies: BTC, ETH, XRP and BNB. The results are estimated using the 1% quantile.

Table 7 Comparing the results of Expected shortfall (CVaR) measure among methods for the 5% quantile

	BTC	ETH	XRP	BNB
Optimal Coupling	-9.825	-13.128	-21.345	-17.045
Historical Simulation	-12.479	-15.164	-16.494	-15.805
Monte Carlo	-8.755	-10.602	-10.815	-9.699
Variance Covariance	-	-	-	-

Note: This table reports the results of Expected shortfall (CVaR) for the methods of Optimal Coupling, Historical Simulation, Monte Carlo and Variance Covariance for the following cryptocurrencies: BTC, ETH, XRP and BNB. The results are estimated using the 5% quantile.

4.2.1 Computational Cost

Estimation time is one of the most important aspects to consider when estimating risk measures. The computational cost for each method is summarized in Table 9. Note that the optimal coupling approach takes approximately 10502.6 times longer than the Monte Carlo simulation, which is the slowest of the univariate methods.

Table 8 Comparing the results of Expected shortfall (CVaR) measure among methods for the 1% quantile

	BTC	ETH	XRP	BNB
Optimal Coupling	-11.245	-13.535	-21.162	-17.170
Historical Simulation	-17.405	-18.213	-21.714	-17.212
Monte Carlo	-13.006	-15.626	-17.589	-16.353
Variance Covariance	-	-	-	-

Note: This table reports the results of Expected shortfall (CVaR) for the methods of Optimal Coupling, Historical Simulation, Monte Carlo and Variance Covariance for the following cryptocurrencies: BTC, ETH, XRP and BNB. The results are estimated using the 1% quantile.

The estimated cost involved in the Optimal Coupling method does not depend on the dimension of the data (d). An important point highlighted by Bercu et al. (2023) is that the estimates of Monge's maps can suffer from the curse of dimensionality. However, when the entropic map is the objective function, the convergence rates are independent of d for any $\epsilon > 0$.

Table 9 Computational Cost

	Time in seconds
Optimal Coupling	84489.054
Historical Simulation	0.002
Monte Carlo	8.045
Variance Covariance	0.001

4.2.2 Backtesting

The previous section's results were derived from a sample spanning from July 2, 2021, to September 13, 2022. We will now proceed to examine the comparative efficacy of risk calculation methods, comparing Optimal Transport measures and the traditional approaches, through a backtesting procedure. This analysis will utilize data from September 14, 2022, to December 31, 2022, to evaluate the performance of these risk measures.

To assess the accuracy of the model, backtesting analysis and tests were conducted for Value at Risk (VaR) measures. The analyzes performed include calculating the empirical violation rate, the Kupiec test and binomial distribution test.

Let us define the violations, $I_t(\alpha)$, as

$$I_t(\alpha) = \begin{cases} 1 & \text{if } \; x_t \leq VaR_{\alpha,t} \\ 0 & \text{if } \; x_t > VaR_{\alpha,t} \end{cases} \tag{31}$$

The empirical measure of violation rate measures whether the number of VaR violations is close to the expected value, which is defined by the VaR size.

Therefore, at a VaR of 5%, a number of violations is expected in 5% of the sample.

The rate of violations observed in the backtesting sample is a point measure of the performance of the VaR calculation methods. A formal test to verify whether empirical violations are compatible with the expected violation rate is the Kupiec test (Zhang and Nadarajah, 2018). The Kupiec statistic, which tests whether the proportion of violations (POF) $100\hat{\alpha}$ is equal to 100α, is given as follows.

$$\text{POF} = 2\ln\left[\left(\frac{1-\hat{\alpha}}{1-\alpha}\right)^{n-I(\alpha)}\left(\frac{\hat{\alpha}}{\alpha}\right)^{I(\alpha)}\right], \tag{32}$$

where $\hat{\alpha} = \frac{1}{n}I(\alpha)$ and $I(\alpha) = \sum_{t=1}^{n} I_t(\alpha)$, assuming a Likelihood Ratio form. Note that if the model is well adjusted, the test statistic will be zero. However, if the proportion of violations is different from 100α, the test statistic will increase, indicating that the model can underestimate or overestimate the level of risk.

The Binomial distribution test is an extension of the independence test proposed by Christoffersen (1998). According to Zhang and Nadarajah (2018), if violations $I_t(\alpha)$, are independently and identically distributed and also $\Pr[I_{t+1}(\alpha) = 1] = \alpha$, then the total number of violations H, follows a binomial distribution $B(n, \alpha)$, where the mean of H, denoted as $E(H)$, is equal to $n\alpha$, and the variance of H, denoted as $Var(H)$, is equal to $n\alpha(1-\alpha)$. As Zhang and Nadarajah (2018) add, when the number of observations is large enough, the central limit theorem can approximate the binomial distribution by the normal distribution.

Analyzing the violation rate results for the 5% and 1% estimates of VaR, shown in Tables 10 and 11, we see that the Optimal Coupling and Historical Simulations methods have the lowest failure ratios. For VaR(5%) only the Monte Carlo and Variance Covariance methods for the ETH series show a violation rate close to expected for the ETH series at $\alpha = 5\%$. For VaR(1%), the Optimal Coupling and Historical Simulation methods generally demonstrate lower violation rates, with most cryptocurrencies remaining within the expected threshold. The Monte Carlo method shows similar performance to Optimal Coupling for most cryptocurrencies, but a slightly higher violation rate for XRP. The Variance Covariance method exhibits higher violation rates for some cryptocurrencies, particularly ETH and BNB.

The results for Optimal Coupling model in Kupiec´s test, for 5% quantile (Table 12) are similar to the Historical Simulation method, with the clear exception in XRP. Also, only the VaR measure for ETH computed with Monte Carlo and Variance Covariance methods can not reject the null hypothesis, i.e., the VaR model is adequate in these cases. For the 1% quantile (Table 13), the Optimal Coupling method have low values for ETH and XRP, and the results for BTC and BNB are really close to zero, which means that the model proposed by Bercu et al. (2023) is well adjusted. Also note that all the

Table 10 Violation Rate (%) for VaR at 5% quantile

	BTC	ETH	XRP	BNB
Optimal Coupling	1.835	1.835	0.000	0.917
Historical Simulation	0.917	1.835	1.835	0.917
Monte Carlo	1.835	4.587	1.835	1.835
Variance Covariance	1.835	4.587	1.835	1.835

Note: This table reports the violation rate (%) for VaR of BTC, ETH, XRP and BNB at 5% quantile for following methods: Optimal Coupling, Historical Simulation, Monte Carlo and Variance Covariance.

Table 11 Violation Rate (%) for VaR at 1% quantile

	BTC	ETH	XRP	BNB
Optimal Coupling	0.917	1.835	0.000	0.917
Historical Simulation	0.000	0.917	0.000	0.917
Monte Carlo	0.917	1.835	1.835	0.917
Variance Covariance	1.835	2.752	1.835	1.835

Note: This table reports the violation rate (%) for VaR of BTC, ETH, XRP and BNB at 1% quantile for following methods: Optimal Coupling, Historical Simulation, Monte Carlo and Variance Covariance.

Fig. 3 Violations of the returns (Optimal Coupling method).

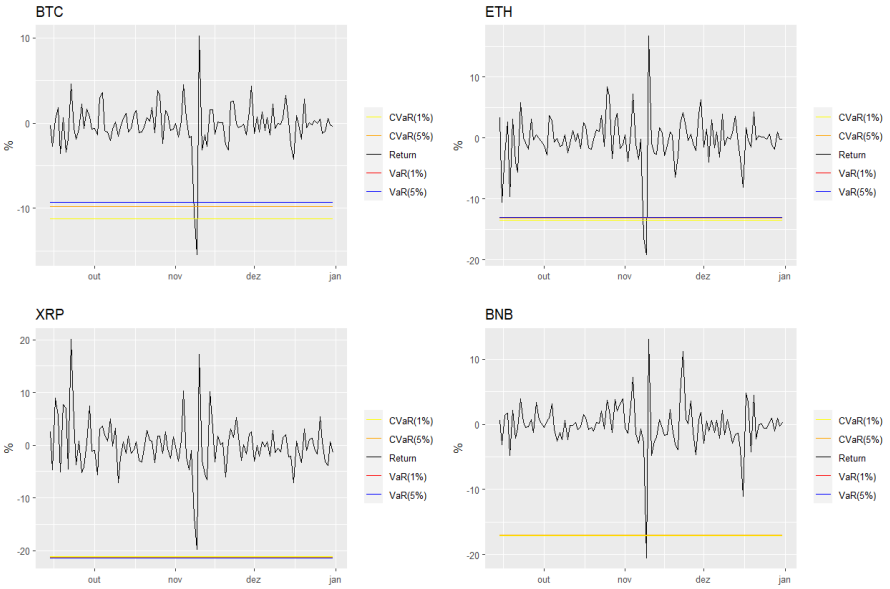

results in Table 13 cannot reject the null hypothesis, which suggests that for all cryptocurrencies, the models fit the tail risk dynamics well.

We present the results of the Binomial test in Tables 14 and 15. The results indicate that, for the 5% quantile and for all cryptocurrencies, the Monte Carlo and Variance Covariance methods do not reject the null hypothesis that $H_0 : \mathrm{E}[I_t(\alpha)] = n\alpha$. Also, the null hypotheses cannot be rejected for ETH and

Table 12 Kupiec's Test for VaR at 5% quantile

	BTC	ETH	XRP	BNB
Optimal Coupling	3.004*	3.004*	11.182***	5.697**
Historical Simulation	5.697**	3.004*	3.004*	5.697**
Monte Carlo	3.004*	0.04	3.004*	3.004*
Variance Covariance	3.004*	0.04	3.004*	3.004*

Note: This table reports the results of the Kupiec´s Test for VaR of BTC, ETH, XRP and BNB at 5% quantile for following methods: Optimal Coupling, Historical Simulation, Monte Carlo and Variance Covariance. The p-values are represented for $^{***}p < 0.01$ $^{**}p < 0.05$ and $^{*}p < 0.10$.

Table 13 Kupiec's Test for VaR at 1% quantile

	BTC	ETH	XRP	BNB
Optimal Coupling	0.008	0.616	2.191	0.008
Historical Simulation	2.191	0.008	2.191	0.008
Monte Carlo	0.008	0.616	0.616	0.008
Variance Covariance	0.616	2.289	0.616	0.616

Note: This table reports the results of the Kupiec´s Test for VaR of BTC, ETH, XRP and BNB at 1% quantile for following methods: Optimal Coupling, Historical Simulation, Monte Carlo and Variance Covariance. The p-values are represented for $^{***}p < 0.01$ $^{**}p < 0.05$ and $^{*}p < 0.10$.

XRP using the Historical Simulation method and for BTC and ETH using the Optimal Coupling method, i.e. the number of violations is consistent with the expected 5% violation rate for these cryptocurrencies when VaR is measured using these methods. For the 1% quantile, only the VaR measure for ETH with Variance Covariance rejects the null hypothesis.

Table 14 Binomial Test for VaR at 5% quantile

	BTC	ETH	XRP	BNB
Optimal Coupling	2	2	0***	1**
Historical Simulation	1**	2	2	1**
Monte Carlo	2	5	2	2
Variance Covariance	2	5	2	2

Note: This table reports the statistics (number of successes) of the Binomial Test for VaR of BTC, ETH, XRP and BNB at 5% quantile for following methods: Optimal Coupling, Historical Simulation, Monte Carlo and Variance Covariance. The hypotheses are $H_0 : \mathrm{E}[I_t(\alpha)] = n\alpha$ vs $H_1 : \mathrm{E}[I_t(\alpha)] \neq n\alpha$. The number of trials is 109. The p-values are represented for $^{***}p < 0.01$ $^{**}p < 0.05$ and $^{*}p < 0.10$.

5 Conclusion

In this article, we analyze a new class of tail risk measures proposed by Bercu et al. (2023), which is based on the Optimal Coupling Method, in the analysis of the cryptocurrency market, comparing with some usual static measures of tail risk based on univariate estimation (Monte Carlo Simulation, His-

Table 15 Binomial Test for VaR at 1% quantile

	BTC	ETH	XRP	BNB
Optimal Coupling	1	2	0	1
Historical Simulation	0	1	0	1
Monte Carlo	1	2	2	1
Variance Covariance	2	3*	2	2

Note: This table reports the statistics (number of successes) of the Binomial Test for VaR of BTC, ETH, XRP and BNB at 1% quantile for following methods: Optimal Coupling, Historical Simulation, Monte Carlo and Variance Covariance. The hypotheses are $H_0 : \mathrm{E}[I_t(\alpha)] = n\alpha$ vs $H_1 : \mathrm{E}[I_t(\alpha)] \neq n\alpha$. The number of trials is 109. The p-values are represented for $^{***}p < 0.01$ $^{**}p < 0.05$ and $^{*}p < 0.10$.

torical Simulation, and Variance-Covariance methods), in terms of magnitude, computational time, and backtesting results.

We evaluated both the traditional univariate measures and the novel measures on the cryptocurrency market (BTC, ETH, XRP, and BNB), renowned for its exceptionally high risks and returns compared to other investment markets. Across all quantiles analyzed, the Optimal Coupling and Historical Simulation methods consistently exhibit the highest Value at Risk (VaR) and Expected Shortfall (CVaR) measures in absolute terms.

However, similar to other univariate risk methods commonly favored by market analysts, the Historical Simulation approach overlooks the inherent risk correlation structure between the components of a random vector. This neglect can lead to incomplete risk assessments, especially in complex and interconnected markets such as cryptocurrency.

Regarding the backtesting results, it is interesting to note that the results of the Optimal Coupling method at the 1% quantile are slightly better when compared to the results obtained at the 5% quantile and, in some cases, the backtesting results shows that Optimal Coupling has more precision estimates than the univariate measures (at the 1% quantile).

The theory of Optimal Transport, along with the recent work of Bercu et al. (2023), introduces a novel multivariate approach that has seen limited use in financial markets for calculating risk measures. According to Hallin et al. (2021), center-outward quantile contours are robust indicators in the multivariate context of risk management measures.

One relevant aspect of the technique proposed by Bercu et al. (2023) is the characteristics of Monge-Kantorovich quantiles, which eliminate the need for assumptions about the distribution's tail or a full parametric model. This stems from the inherent flexibility of Monge-Kantorovich quantiles to adapt the distribution's shape accordingly.

The primary challenge addressed in this paper, as well as in the Optimal Transport literature, as noted by Carlier et al. (2016), lies in establishing a deterministic mapping that effectively transforms one probability distribution to another. However, the advantage of not requiring any assumptions about the distribution's tail comes with a trade-off: increased computational cost. The required time, measured in seconds, exceeds that of univariate methods,

reaching up to approximately 10502.6 times longer than the Monte Carlo simulation method, which is the slowest among univariate approaches.

Furthermore, an essential observation emphasized by both Bercu et al. (2023) and de Valk and Segers (2018a) is that the spherical uniform U_d may not ensure stability of the quantile map as it extends into the tail contours. Therefore, as suggested by Bercu et al. (2023), alternative spherical reference measures can be employed to define the center-outward superquantiles. This underscores the method's limitations in certain applications and highlights the need for refinement to accommodate turbulent scenarios and more volatile markets.

Declarations

Funding: The authors acknowledge funding from Capes, CNPq (310646/2021-9) and FAPESP (2023/02538-0).
Competing Interests: The authors have no relevant financial or non-financial interests to disclose.
Author Contributions: The authors contributed equally to all stages of the work.

References

Acerbi, C. and Tasche, D. (2002). On the coherence of expected shortfall. *Journal of Banking & Finance*, 26(7):1487–1503.

Akhtaruzzaman, M., Boubaker, S., Nguyen, D. K., and Rahman, M. R. (2022). Systemic risk-sharing framework of cryptocurrencies in the covid–19 crisis. *Finance Research Letters*, 47:102787.

Beirlant, J., Buitendag, S., Del Barrio, E., Hallin, M., and Kamper, F. (2020). Center-outward quantiles and the measurement of multivariate risk. *Insurance: Mathematics and Economics*, 95:79–100.

Bercu, B. and Bigot, J. (2021). Asymptotic distribution and convergence rates of stochastic algorithms for entropic optimal transportation between probability measures.

Bercu, B., Bigot, J., and Thurin, G. (2023). Monge-kantorovich superquantiles and expected shortfalls with applications to multivariate risk measurements. *arXiv preprint arXiv:2307.01584*.

Borri, N. (2019). Conditional tail-risk in cryptocurrency markets. *Journal of Empirical Finance*, 50:1–19.

Bosc, D. and Galichon, A. (2014). Extreme dependence for multivariate data. *Quantitative Finance*, 14(7):1187–1199.

Brenier, Y. (1991). Polar factorization and monotone rearrangement of vector-valued functions. *Communications on pure and applied mathematics*, 44(4):375–417.

Cai, J., Jia, H., and Mao, T. (2022). A multivariate cvar risk measure from the perspective of portfolio risk management. *Scandinavian Actuarial Journal*, 2022(3):189–215.

Carlier, G., Chernozhukov, V., and Galichon, A. (2016). Vector quantile regression: An optimal transport approach. *The Annals of Statistics*, 44(3):1165 – 1192.

Chaim, P. and Laurini, M. P. (2018). Volatility and return jumps in bitcoin. *Economics Letters*, 173:158–163.

Chaim, P. and Laurini, M. P. (2019a). Is bitcoin a bubble? *Physica A: Statistical Mechanics and its Applications*, 517:222–232.

Chaim, P. and Laurini, M. P. (2019b). Nonlinear dependence in cryptocurrency markets. *The North American Journal of Economics and Finance*, 48:32–47.

Chaudhuri, P. (1996). On a geometric notion of quantiles for multivariate data. *Journal of the American statistical association*, 91(434):862–872.

Christoffersen, P. F. (1998). Evaluating interval forecasts. *International Economic Review*, 39(4):841–862.

Cousin, A. and Di Bernardino, E. (2013). On multivariate extensions of value-at-risk. *Journal of Multivariate Analysis*, 119:32–46.

Cousin, A. and Di Bernardino, E. (2014). On multivariate extensions of conditional-tail-expectation. *Insurance: Mathematics and Economics*, 55:272–282.

Cuturi, M. (2013). Sinkhorn distances: Lightspeed computation of optimal transport. *Advances in neural information processing systems*, 26.

Danielsson, J. (2011). *Financial risk forecasting: The theory and practice of forecasting market risk with implementation in R and Matlab*. John Wiley & Sons.

de Valk, C. and Segers, J. (2018a). Stability and tail limits of transport-based quantile contours. Technical report, arXiv preprint arXiv:1811.12061.

de Valk, C. and Segers, J. (2018b). Tails of optimal transport plans for regularly varying probability measures. Technical report, arXiv preprint arXiv:1811.12061.

Del Barrio, E., González-Sanz, A., and Hallin, M. (2019). A note on the regularity of center-outward distribution and quantile functions. Technical report, arXiv preprint arXiv:1912.10719.

Ekeland, I., Galichon, A., and Henry, M. (2012). Comonotonic measures of multivariate risks. *Mathematical Finance: An International Journal of Mathematics, Statistics and Financial Economics*, 22(1):109–132.

Embrechts, P. (2000). Extreme value theory: Potential and limitations as an integrated risk management tool. *Derivatives Use, Trading & Regulation*, 6(1):449–456.

Galichon, A. (2017). A survey of some recent applications of optimal transport methods to econometrics. *The Econometrics Journal*, 20(2):C1–C11.

Galichon, A. (2018). *Optimal transport methods in economics*. Princeton University Press.

Genevay, A. (2019). *Entropy-regularized optimal transport for machine learning*. PhD thesis, Paris Sciences et Lettres (ComUE).

Genevay, A., Cuturi, M., Peyré, G., and Bach, F. (2016). Stochastic optimization for large-scale optimal transport. *Advances in neural information processing systems*, 29.

Ghosal, P. and Sen, B. (2022). Multivariate ranks and quantiles using optimal transport: Consistency, rates and nonparametric testing. *The Annals of Statistics*, 50(2):1012–1037.

Hallin, M., del Barrio, E., Cuesta-Albertos, J., and Matrán, C. (2021). Distribution and quantile functions, ranks and signs in dimension d: A measure transportation approach. *The Annals of Statistics*, 49(2):1139 – 1165.

Hallin, M., Hlubinka, D., and Hudecová, Š. (2023). Efficient fully distribution-free center-outward rank tests for multiple-output regression and manova. *Journal of the American Statistical Association*, 118(543):1923–1939.

Hallin, M., Paindaveine, D., and Šiman, M. (2010). Multivariate quantiles and multiple-output regression quantiles: From L1 optimization to halfspace depth. *The Annals of Statistics*, 38(2):635 – 669.

Heffernan, J. E. and Tawn, J. A. (2004). A conditional approach for multivariate extreme values (with discussion). *Journal of the Royal Statistical Society Series B: Statistical Methodology*, 66(3):497–546.

Jlassi, N. B., Jeribi, A., Lahiani, A., and Mefteh-Wali, S. (2023). Subsample analysis of stock market – cryptocurrency returns tail dependence: A copula approach for the tails. *Finance Research Letters*, 58:104056.

Jorion, P. (1996). Risk2: Measuring the risk in Value at Risk. *Financial Analysts Journal*, 52(6):47–56.

Kantorovich, L. (1942). On the transfer of masses (in russian). In *Doklady Akademii Nauk*, volume 37, page 227.

Koenker, R. (2005). *Quantile Regression*. Econometric Society Monographs, Cambridge.

Koltchinskii, V. I. (1997). M-estimation, convexity and quantiles. *The Annals of Statistics*, 25(2):435 – 477.

Lahiri, S. N. (2003). *Resampling Methods for Dependent Data*. Springer Series in Statistics. Springer New York, NY.

Liu, R. Y. (1990). On a Notion of Data Depth Based on Random Simplices. *The Annals of Statistics*, 18(1):405 – 414.

McCann, R. J. (1995). Existence and uniqueness of monotone measure-preserving maps. *Duke Mathematical Journal*, 80(2):309 – 323.

Mensi, W., Gubareva, M., Ko, H. U., et al. (2023). Tail spillover effects between cryptocurrencies and uncertainty in the gold, oil, and stock markets. *Financial Innovation*, 9:92.

Naeem, M., Bouri, E., Boako, G., and Roubaud, D. (2020). Tail dependence in the return-volume of leading cryptocurrencies. *Finance Research Letters*, 36:101326.

Oja, H. (1983). Descriptive statistics for multivariate distributions. *Statistics & Probability Letters*, 1(6):327–332.

Prékopa, A. (2012). Multivariate value at risk and related topics. *Annals of Operations Research*, 193(1):49–69.

Robbins, H. and Monro, S. (1951). A Stochastic Approximation Method. *The Annals of Mathematical Statistics*, 22(3):400 – 407.

Rockafellar, R. T. and Royset, J. O. (2013). Superquantiles and their applications to risk, random variables, and regression. In *Theory Driven by Influential Applications*, pages 151–167. Informs.

Rockafellar, R. T. and Royset, J. O. (2018). Superquantile/cvar risk measures: Second-order theory. *Annals of Operations Research*, 262:3–28.

Rockafellar, R. T., Royset, J. O., and Miranda, S. I. (2014). Superquantile regression with applications to buffered reliability, uncertainty quantification, and conditional value-at-risk. *European Journal of Operational Research*, 234(1):140–154.

Shayya, R., Sorrosal-Forradellas, M. T., and Terceño, A. (2023). Value-at-risk models: a systematic review of the literature. *Journal of Risk*, 25(4).

Torres, R., Lillo, R. E., and Laniado, H. (2015). A directional multivariate value at risk. *Insurance: Mathematics and Economics*, 65:111–123.

Vieira, L. I. and Laurini, M. P. (2023). Time-varying higher moments in bitcoin. *Digit Finance*, 5:231–260.

Zhang, Y. and Nadarajah, S. (2018). A review of backtesting for Value at Risk. *Communications in Statistics-Theory and methods*, 47(15):3616–3639.

Zuo, Y. (2003). Projection-based depth functions and associated medians. *The Annals of Statistics*, 31(5):1460–1490.